UNIVERSIDAD DE CHILE
FACULTAD DE CIENCIAS FÍSICAS Y MATEMÁTICAS
DEPARTAMENTO DE INGENIERÍA MATEMÁTICA

ALLEN-CAHN EQUATION AS A MODEL FOR PHASES OF APPLE CHIMERA

MEMORIA PARA OPTAR AL TÍTULO DE INGENIERO CIVIL MATEMÁTICO

ANTOINE MARULLAZ

PROFESOR GUÍA:
MICHAŁ KOWALCZYK

MIEMBROS DE LA COMISIÓN:
GABRIELLE NORNBERG
SEBASTIÁN DONOSO FUENTES

SANTIAGO DE CHILE
2022

ECUACIÓN DE ALLEN-CAHN COMO MODELO PARA FASES DE MANZANAS CHIMERAS

El objetivo del presente trabajo es encontrar un modelo matemático que pueda encajar un fenómeno biológico poco común y sorprendente: el quimerismo.

Para ello pretendemos utilizar la ecuación de Allen-Cahn sobre la transición de fase peculiar del color de manzanas quiméricas. Por lo tanto, después de haber introducido la ecuación, nos esforzamos demostrar la pertinencia de tal elección para modelar el fenómeno. Para eso introducimos conceptos genéticos subyacentes, y hacemos hipótesis adecuadas. Luego desarrollamos el modelo mediante cálculos con el fin de obtener soluciones comparables a la realidad. En la ultima parte discutimos la validad del modelo relacionando esas soluciones con varios ejemplos observados, lo cual nos permite afinar el modelo y proponer ejes de desarrollo futuros.

Por ende el trabajo consiste en construir un modelo matemático de principio a fin aplicado a la biología, comprobando como corresponde varias etapas científicas.

Table of Content

1   Introduction

On very rare occasions, one can encounter bi-colour apples with surprisingly regular and precise separation between the two colours (Figure 1). Those occurrences are possible due to the genetic instability of apples on one hand, and the techniques used to farm them on the other hand. Although such apples may be mistaken as simply having a particular genetic trait regarding their coloured skin, they are actually individual examples of a long known biological anomaly called *chimera*, which specifically combines two sets of distinct genetic materials.

After having introduced the biological background to understand such phenomenon and the technical aspects of the apple case, we will propose a mathematical model to fit the phase transition of the colour of the skin on a chimera apple using the famous Allen-Cahn equation. We firstly draw a quick introduction to this equation and then justify the use of such a model by studying the genetic dynamics in action during the apparition of a chimera. Later we specify the model and apply it on a 2-sphere. Finally we will discuss the model on other sphere-like surfaces and compare our results to various observations of chimeras to discuss its validity and limits.
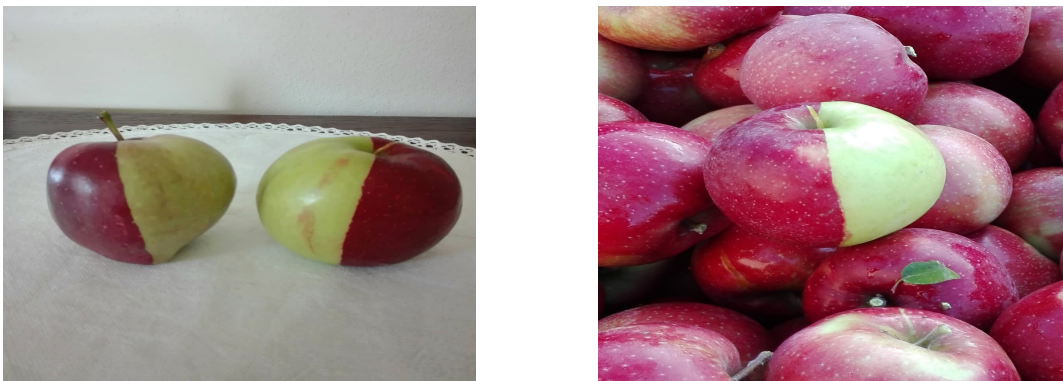

Figure 1: Red/Green phase transition on two apples

2   Biological background

Multi-cellular organisms are usually composed by cells sharing the same genotype which means the same genetic material. Two different organisms can generate a new one by mixing their genome, and the resulting organism is called a hybrid. A hybrid has a phenotype which express characteristic traits of both its parents, however each one of its cells contains the same genome: the mix of the genomes of its parents. In contrast, a chimera is a single organism composed of cells with more than one distinct genotype. Hence a chimera also expresses traits of both its parents but independently from one another. As for the apple or for other examples (see below), the organism might show patches of cells or division between external and interior tissues which have separately the exact same genome of one of the chimera's parents ([TB92]).

In any type of plants, the buds are organized structures protected by scales. The terminal part, or meristem, is in the form of a dome where the cells are subjected to numerous divisions to give new axillary vegetative shoots or to transform into an inflorescence. The cell divisions, which occur by mitosis, give cells whose genetic heritage is identical to that of the cell which gave birth to them. This process is usually regular but it can be disturbed by natural or induced mutations.

Figure 2: A rose chimera : red part's cells have the exact same genome has the chimera's red parent.

The grafting process used in the progressive domestication of food is the major factor that can lead to the creation of chimeras in domesticated plants: it appears commonly in leaves, flowers or fruits such as apples. It consists in joining tissues of two different plants, with different qualities, in order for them to grow together. The upper part of the combined plant is called the scion while the lower part is called the rootstock. In the case of growing apples for example, we might want to select an apple tree which is sturdy and grows evenly as the rootstock, even though it does not produce necessarily good quality fruits. To that rootstock can then be grafted as a scion a part from a tree that specifically grows fruits with superior quality and taste or with any interesting attribute desired. It can already be envisioned that the chimeral fruits created from a graft will feature cells containing the genome of the rootstock as well as cells with the genome from the scion ([FC16]).

In 1674, Pietro Nati (1625–1685), director of the Botanical Garden of the University of Pisa, published *De malo limonia citrata-aurantia vulgo la bizzarria* (On the citron-orange lemon, called the bizzarria), in which he described a lemon-orange "graft chimera" a tree that bears oranges, lemons, and citrons and combinations of those. It is the first reported non-mythological chimera. Its leaves and flowers are also a mixture of different citrus. The case of apples we are studying are also "graft chimera".

Figure 3: Bizzaria : a famous fruit chimera.

As one can see in the figure below it stems from two fairly different fruits, namely the Florentine citron and sour orange. Apart from being the most famous instance of plant chimera, the bizzaria interest us in particular because it comes from the same grafting process as the apple one. Both fruit results of this widely-used fruit farming technique. In the third section we show why this technique in particular serves as a good theoretical support for our model. The figure below highlights the difference between a chimera (right) and what a 'normal' hybrid' should look like - a uniform genetic mix of both of its parents.
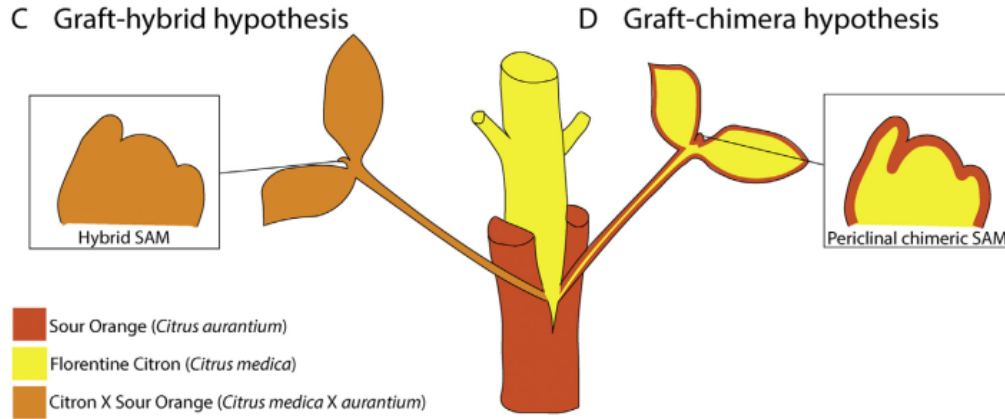
Figure 4: Two hypothesis two explain the unusual scion. Figure from [FC16]

3 Allen-Cahn equation

3.1 Introduction and notations

The Allen-Cahn equation is a reaction-diffusion equation popularized by Sam Allen and John W. Cahn in [CA77]. It is often used to model the change in space and time of the concentration of two chemical substances. The equation is as follow :

$$\Delta u + F'(u) = \frac{\partial u}{\partial t}$$

Where u is a scalar function representing the state of the mixture for any point in the studied space containing the materials, with $u = \pm 1$ being the two pure phases. And F is a double-well potential, with equal depth at 1 and -1.

The additional parameter ϵ is put in the equation to scale its solution in space and time. Namely, a smaller epsilon will induce slower change of the scalar function u, as well as a thinner interface between the two phases. The modified equation is written :

$$\epsilon^2 \Delta u + F'(u) = \frac{\partial u}{\partial t}$$

Classic examples of application of the Allen-Cahn equation are the description of concentration of two metal substances in an alloy, or interface between ice and water in a closed system. In the figure 5 below for instance, red points in the plane correspond to pure phase of one metal and blue ones to the other.
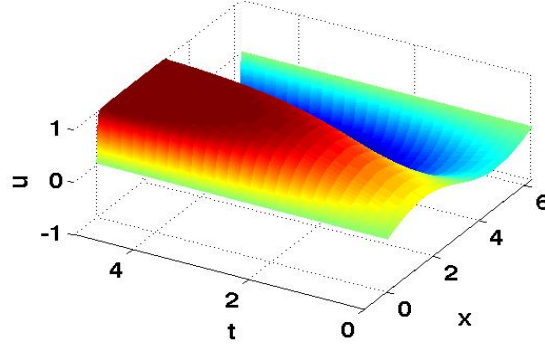
Figure 5: , from [wika]

3.2   Some analytical solutions in 1 & 2 dimensions

A first interesting approach to this equation is to look for stationary solutions, which means, u solutions to the equation :

$$\epsilon^2 \Delta u + F'(u) = 0$$

Those solutions characterize the feasible mixtures that would theoretically not vary over time. We shall here look at a few instances where we can explicit stationary solutions and in the next section justify they might fit our problem.

Primarily let's look at the equation in one dimension. From now on we will use an often used double well function :

$$F = \frac{1}{4}(1 - u^2)^2$$

In this section to alleviate the notation we will take $\epsilon = 1$. The equation is now a simple ordinary differential equation :

$$u'' + u - u^3 = 0$$

Now let $W(u) = \frac{1}{4}(1 - u^2)^2$ so that :

$$W'(u) = u - u^3$$

Then we notice that :

$$\frac{d}{dx}(u'(x)^2 - 2W(u(x))) = 2u'(x)u''(x) - 2u'(x)W'(u(x)) = 0$$

Thus $u'(x)^2 = 2W(u(x)) + \lambda$ for some $\lambda \in \mathbb{R}$

We begin by looking for any solution. For example if $\lambda = 0$ and we suppose $u'(x)^2 \geq 0$ we can solve the equation :

$$\frac{du}{dx} = \frac{1}{\sqrt{2}}(1 - u^2)$$

We can separate the variables in this equation :

$$\frac{du}{1 - u^2} = \frac{dx}{\sqrt{2}}$$

Then

4

$$\int \frac{du}{(1-u)(1+u)} = \int \frac{dx}{\sqrt{2}}$$

That is a simple partial fraction decomposition :

$$\int \frac{du}{2(1-u)} + \frac{du}{2(1-u)} = \frac{x}{\sqrt{2}} + x_0$$

Finally we get :

$$-\frac{\ln(1-u)}{2} + \frac{\ln(1+u)}{2} = \frac{x}{\sqrt{2}} + x_0$$

$$\ln\left(\sqrt{\frac{1+u}{1-u}}\right) = \frac{x}{\sqrt{2}} + x_0$$

which has solutions $u(x) = H(x - x_0) = \tanh(\frac{x-x_0}{\sqrt{2}})$ where $x_0 \in \mathbb{R}$ arbitrary, which is called the heteroclinic solution, and $u = \pm 1$. One can check by differentiating that $H(x)$ is indeed a solution to the stationary Allen-Cahn equation at dimension 1.
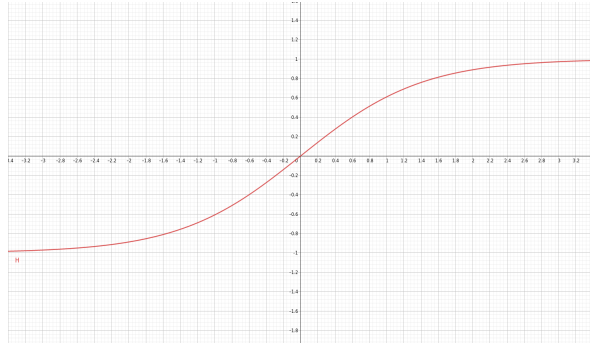

Figure 6: The heteroclinic solution in dimension 1

Now we will show that a solution u to the 1-dimensional Allen-Cahn equation has finite energy if and only if $u(x) = \pm H(x - x_0)$ or ± 1.

We have already seen that $u'(x)^2 = 2W(u(x)) + \lambda$ for $\lambda \in \mathbb{R}$. But since :

$$\int_{-\infty}^{+\infty} \frac{1}{2} u'(x)^2 + W(u(x))\, dx < \infty$$

and since both terms are non-negative, there exist a sequence $x_k \to \infty$ such that $u'(x_k) \to 0$ and $W(u(x_k)) \to 0$. Thus,

$$u'(x_k) - 2W(u(x_k)) \to 0$$

which implies that λ is equal to 0 as well, so we are back to the calculations done in the previous paragraph. This concludes the analysis of stationary solutions in one dimension.

Obviously Allen-Cahn's equation generalizes to higher dimensions and a lot of research has been done to characterize its analytical solutions under various conditions. We will now expose a few analytical solutions in dimension 2 and results in higher dimension before linking the equation to our specific problem.

We can first observe that the one dimensional solution $H(x)$ we considered before provides a solution on $\mathbb{R}^2$ as well. To that end, fixing $a \in \mathbb{R}^2$ and $b \in \mathbb{R}$ we simply consider the function :

$$u(x) = H(\langle a, x \rangle - b).$$

u can be derived to check that it solves the equation. We can note too that this solution has flat level and hence its nodal set $u = 0$ is a straight line perpendicular to a and scaled by b. Effectively this solution scales up to higher dimensions (see [Cho19], [Gui]) and interestingly it is known to be the only smooth bounded monotonous in one direction solution of the Allen-Cahn equation up to dimension 8 according to De Giorgi's conjecture ([dPKW11]).

Obviously, by relaxing the condition the space of solution is much greater and still studied nowadays. For example one can construct 2k ends solutions ([KLPW14]) in the plane like the figure below :
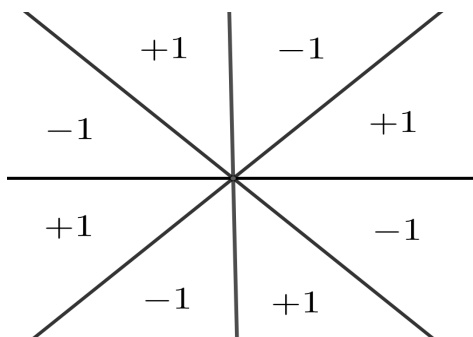

Figure 7

For more information detailed results on complete solutions in higher dimensions see [dPKPW10], [KLP12], [dP]. What interest us and has to be kept in mind for the rest of the study is that in two dimensions, the stationary solutions minimizing energy have necessarily straight lines as nodal set. In our case we will try to model the colour variation on the skin of apples chimera. To that end in the following section we will explicit our model as well as explain why we look for stationary solutions, why they should minimize the energy and what would the equivalent of "straight lines" be on our apples.

4   The model for apple chimeras

4.1   Justifying the model : genetic potential

Following what has been said in the biological background, chimeras based on the structure of the meristem may be classified in different types of divisions: sectoral (a wedge of tissue), mericlinal (a wedge of tissue in one or more layers of the meristem), and periclinal, (hand-in-glove type) confined to one or more layers of the meristem. The periclinal chimeras are stable. For mericlinal chimeras, like our apple case, the mutated tissue has invaded the peripheral layers of the meristem and in particular the cell layer that leads to the formation of the epidermis, as for periclinal chimeras, except that the peripheral mutation covers only a part of the meristem. These chimeras are very unstable. They can be observed on the epidermis of some fruits where only a part with clear contours is differently colored. The size and frequency of sectoring is a function of transposon activity and the rate of cell division ([NHY92]). A transposon or transposable element is a DNA sequence that can change its position within a genome, sometimes creating or reversing mutations and altering the cell's genetic identity

and genome size. Transposition often results in duplication of the same genetic material.

This concept of transposon is key to our understanding of the model. In the early development phase of the fruit, depending of how "genetically contaminated" from the rootstock the scion is, two type of cells will be generated (see figure below, mericlinical). During growth transposon will act like a genetic potential on neighboring cells : a rootstock cell surrounded by scion cells will most likely make way to scion cells along the growth process and vice versa. Only in the rarer case where originally both type of cells are relatively in equal quantity will the division be maintained over time. Our model tries to find those equilibrium and explain their scarcity in nature.
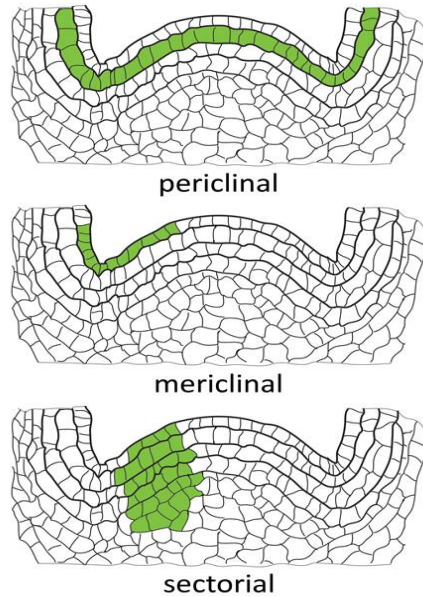

periclinal

mericlinal

sectorial

Figure 8: [lin]

In the case of the apple which is not a flat surface (like a leaf could be considered) but a spherical surface, the case of the division called mericlinal (of unstable type), we envision that it acts as the potentially most stable form of a rubber band which divides the sphere in its middle on the surface of the apple, without intervening in its flesh. It is a constant struggle between cells of one genome on one side and cells of another genome on the other. Each side pushes the boundary or "rubber band" giving it this regular shape observed on our reference photographs initially presented ([GKH$^+$10]).

Based on those biological evidence and our pictures, we see that the line of transition between red and green is very thin, which suggest a very small ϵ, and therefore a fast characteristic time of transition. This justify the very low frequency of appearance of chimeras : except for apples initially very close to the equilibrium, most apples get enough time for one of the cell type to prevail over the other. We will now expose to model to explain mathematically the shape of the boundaries of the surviving apple chimeras.

4.2   The model

We study solutions of the stationary Allen-Cahn equation on a 2-sphere. Green colour is represented as $u = -1$ and red as $u = 1$. The characteristic length of transition from red to green is our variable ϵ. The figure below illustrate a possible solution.

$$\epsilon$$

$$u \approx -1 \ \text{(green)}$$

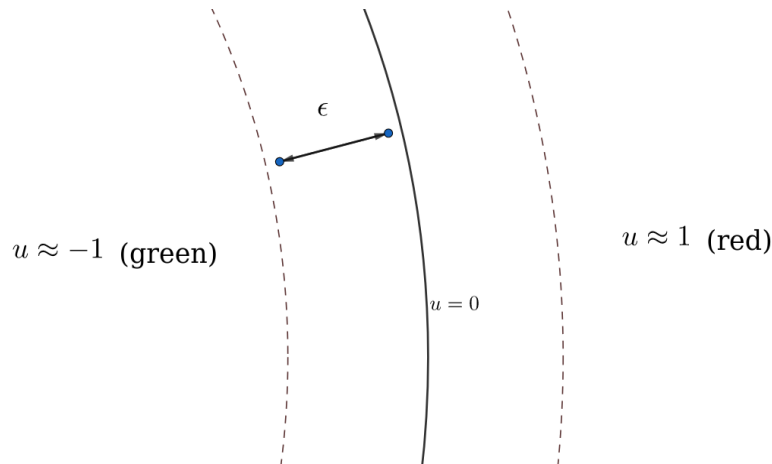$$u \approx 1 \ \text{(red)}$$

$$u = 0$$

Figure 9

5   Looking for geometrical solutions : mean curvature flow

5.1   Calculus for finding the mean curvature flow equation from Allen-Cahn equation on $\mathbb{R}^2$

Rather than trying to explicitly resolve Allen-Cahn solution on a non-plane surface our approach consists in finding a geometric necessary condition for a phase boundary to be stationary. Doing so we can classify which type of lines the colours can draw according to our model, and therefore see if it is always possible and if it fits our observation. Let's first work on the plane to generalize later on other surfaces.

Let γ be the curve defined in our space (here $\mathbb{R}^2$) so that $\gamma(t)$ corresponds to all the points x where $u(x,t) = 0$, that is to say the called above 'boundary between the phases.
We will now try to describe the movement of that curve by using Allen-Cahn equation on u:

$$\epsilon^2 \Delta u + u - u^3 = \frac{\partial u}{\partial t}$$

Given a point x close enough to γ we have the following parameterization for (see Figure 10 below) :

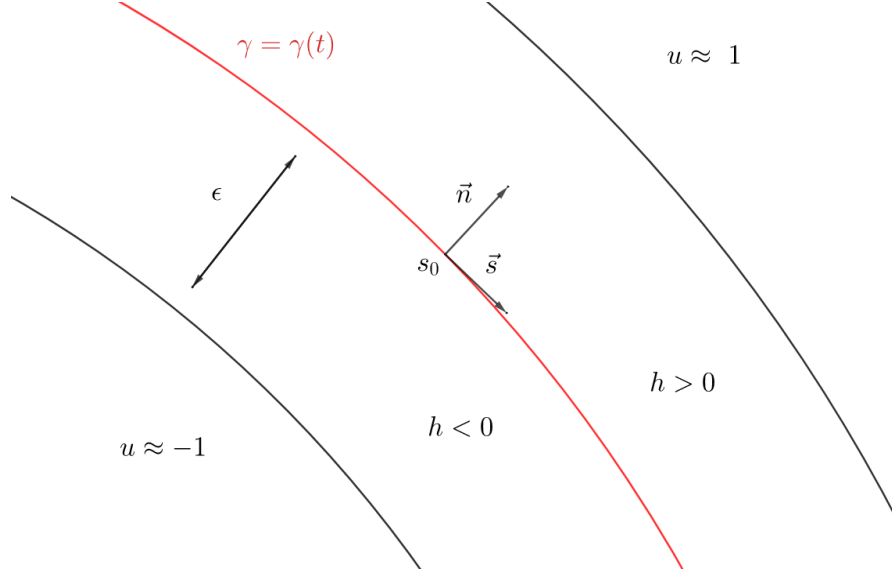$$x(s, h) = \gamma(s) + h\vec{n}(s)$$

Figure 10: schema

For a t given, we approximate $u(x, t)$ at the point x close of $\gamma(t)$:

$$u(t, x) = H\left(\frac{h}{\epsilon}\right) + \phi\left(\frac{h}{\epsilon}, s, t\right)$$

where ϕ is negligible for a small enough h and H is the 1D solution to the equation

$$H(y) = \tanh\left(\frac{y}{\sqrt{2}}\right) \implies H'' + H - H^3 = 0$$

This approximation of u as H perpendicularly from any point of γ is possible for a energy minimizing solution, and it can be obtained from results on Gamma-convergence, see [dPKW11]. So we can calculate the Laplacian for this parameterization using the following formula

$$\Delta = \frac{1}{\sqrt{\det g}}\partial_i(\sqrt{\det g}\, g_{ij}\partial_j)$$

where g is the metric tensor associated to the change of parameter. We have :

$$g_{sh} = g_{hs} = 0 \text{ and } g_{hh} = 1$$

Besides

$$x_s = \partial_s x = \gamma_s(s) + h\vec{n}_s$$

However

$$n_s = -\kappa(s)\gamma_s \text{ and then } x_s = (1 - \kappa h)\gamma_s$$

9

Hence for a parametric curve of speed 1 we finally have : $g_{ss} = (1 - h\kappa)^2$. This way we can apply the Laplacian to our equation :

$$\epsilon^2 \Delta H + \epsilon^2 \Delta \phi + H + \phi - (H + \phi)^3 = H_t + \phi_t$$

$$\Longleftrightarrow \quad \epsilon^2 \Delta H + \epsilon^2 \Delta \phi + H - H^3 + (1 - 3H^2)\phi + N(\phi) = H_t + \phi_t$$

$$\Longleftrightarrow \quad -\frac{\kappa}{1 - h\kappa} H' + \epsilon^2 \Delta \phi + (1 - 3H^2)\phi + N(\phi) = \frac{h_t}{\epsilon} H' + \frac{h_t}{\epsilon} \phi_h + s_t \phi_s + \phi_t$$

$$\Longleftrightarrow \quad \frac{\partial^2 \phi}{\partial h^2} - \frac{\epsilon \kappa}{1 - h\kappa} \frac{\partial \phi}{\partial h} + \frac{\epsilon^2}{1 - h\kappa} \partial_s \left(\frac{1}{1 - h\kappa} \phi_s \right) + (1 - 3H^2)\phi + N(\phi)$$

$$= \left(\frac{\epsilon \kappa}{1 - h\kappa} + \frac{h_t}{\epsilon} \right) H' + \frac{h_t}{\epsilon} \phi_h + s_t \phi_s + \phi_t$$

Finally for ϵ small enough we get the following approximation :

$$\frac{\partial^2 \phi}{\partial h^2} + (1 - 3H^2)\phi \approx \left(\frac{\epsilon \kappa}{1 - h\kappa} + \frac{h_t}{\epsilon} \right) H'$$

Let L be the operator defined as :

$$L : \psi \longrightarrow \frac{\partial^2 \psi}{\partial h^2} + (1 - 3H^2)\psi$$

We notice two things :

$$LH' = 0$$

since

$$H'' + H - H^3 = 0 \implies H''' + H' - 3H^2 H' = 0$$

and also

$$-L\phi \approx \frac{1}{\epsilon} \left(\frac{\epsilon^2 \kappa}{1 - h\kappa} + h_t \right) H'$$

Therefore we have orthogonality between H' and the function $f = \frac{1}{\epsilon}(\frac{\epsilon^2 \kappa}{1 - h\kappa} + h_t)H'$ which translates to

$$\int H'^2 (\epsilon^2 \kappa - h_t) = 0$$

with the changing of variable $y = \frac{h}{\epsilon}$. H' being strictly positive, we get the following necessary condition on h_t :

$$\boxed{\epsilon^2 \kappa = h_t}$$

We can see in that case that for a for a positive curvature relative to a point x, the distance h between x and the boundary γ reduces with time. We recognize a manifestation of the process called the "mean curvature flow" or in two dimensions the "curve-shortening flow" that modifies a smooth

curve by moving its points perpendicularly to the curve at a speed proportional to the curvature (see figure below).
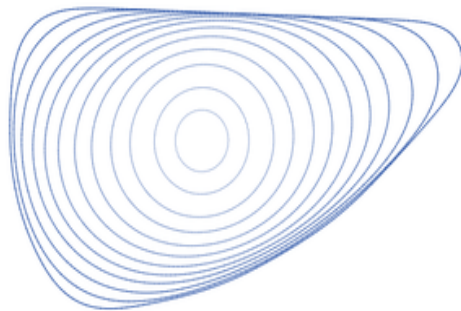

Figure 11: Movement of a curve by curve-shortening flow. The first step is the exterior curve and each iteration correspond to the next inner-curve. [wikb]

Thus, if we want u to be stationary, we need γ to be motionless which implies that if a point x keeps the same value for u the distance h of x to γ must be constant, that is to say $h_s = 0$. From the last result we hence get the condition $\kappa = 0$: the curvature of γ is null in each of its points.
A first remark is that indeed the low-energy solution we mentioned earlier on $\mathbb{R}^2$ had straight line (thus null curvature) as boundaries. We shall now generalise this result to any smooth surface.

5.2   Adapting to other 2-manifolds

Prior to applying the former calculations to other surfaces we must define curvature of a curve on a regular surface in $\mathbb{R}^3$.

Let C be an oriented regular curve contained on an oriented surface S, and $\gamma(s)$ be a parametrization of C, in a neighborhood of $p \in S$, by the arc length s. The algebraic value of the covariant derivative $\left| \frac{D\gamma'(s)}{ds} \right| = \kappa_g$ of $\gamma'(s)$ at p is called the geodesic curvature of C at p. The geodesics which are regular curves are thus characterized as curves whose geodesic curvature is zero.
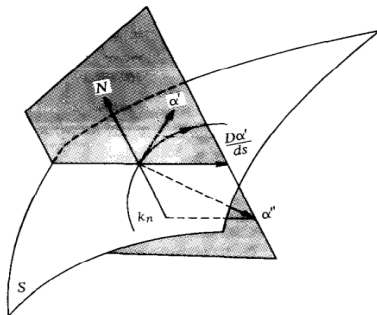

Figure 12: The "overall" curvature vector in $\mathbb{R}^3$ is the sum of the curvature vector of the curve within the surface, and the curvature vector of the surface itself, along the plane perpendicular to the curve. [dC76]

As we can see in the figure above, for a surface embedded in $\mathbb{R}^3$, the geodesic curvature of a curve corresponds to the curvature the curve has in the entire $\mathbb{R}^3$ projected on the tangent space at point p. That same curvature projected along the normal vector at point p is the sectional curvature of the surface in the perpendicular direction of C at point p.
On a general surface we will use the same system of coordinates as in the previous section, with the slight difference that the distance h of our point to the curve will not be along the perpendicular vector

to the curve in $\mathbb{R}^3$ but rather along the only geodesic perpendicular to the curve at the origin. This allow us to put coordinates on points that stay within the surface.

Reiterating the calculation from last section using the geodesic curvature we get the following necessary equation :
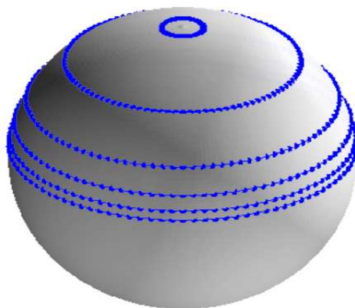
$$\boxed{\epsilon^2 \kappa_g = h_t}$$

Figure 13: [BG10] Theoretically, any curve that does not perfectly fit an equatorial circle will eventually reduce to a point by the process of mean curvature flow. Close to the equator, the curvature is smaller, hence the movement slower.

6   Stationary solutions on other closed non-self-intersecting surfaces

6.1   Existence of a geodesic : the theorem of the three geodesics

Our first example to explain the form of the curve on an apple relates to the famous geodesics of the sphere : the equators. However, a sphere is geometrically a grossly approximation of most apples. A more sensible choice might be a smooth sphere-like surface, that is a smooth surface homeomorphic to (with the same topology as) a 2-sphere. But then what are its geodesics ? More importantly do they even necessarily exist ?

The theorem of the three geodesics states that every Riemannian manifold with the topology of a sphere has at least three closed geodesics that form simple closed curves (i.e without self intersection). For example the figure below depicts a nearly-spherical triaxial ellipsoid which has only three simple closed geodesics, its equators. The theorem is thus sharp. In our case to strengthen our model we can apply our equation on such a surface and we therefore have the existence of at least three geodesics curves on any apple which could support a nodal set of an Allen-Cahn equation solution. To read a demonstration of the three geodesics theorem one can refer for example to [Gra89].
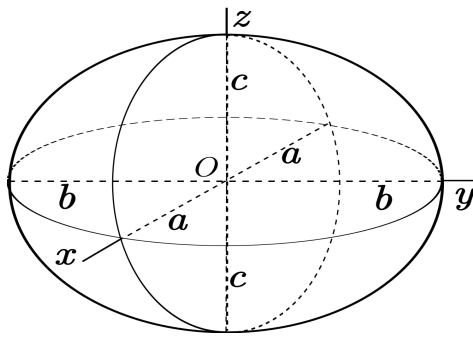
Figure 14: [wikc]

6.2   Discussions

The model being coherent enough we can know compare our results to a few instances of chimeras. Firstly we note that apples from figure 1 seem completely on par with the model : fronteer passes right in the middle of the apples, and even in the case when the apple is rather not spherical (like the left one), the limit passes on the summit of the apple, similarly to the three geodesics of the ellipsoid. The case of the bizzaria depicted below is also very interesting. Indeed our condition on the limit curve does not impose a number of phases restricted to two : stripes can appear combining many equators. More importantly the bizzaria is very coarse and the geodesics appear clearly along the folds : we observe that the phase boundaries seem to follow those geodesics.
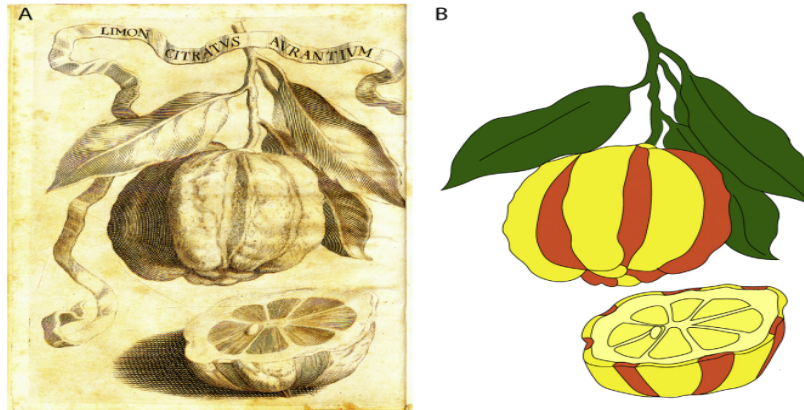

Figure 15:   A and B : original depictions of the bizzaria. C and D : two hypothesis two explain the unusual fruit. Figure from 15

Although harder to assert given the atypical surface the here-under flowers seems to have colour boundaries as plausible geodesics. Further investigation could aim at the confirmation of the model during the growth phase for example to map the trajectory of the curves and see if it fits the curve-shortening flow process. Inferring a coefficient ϵ to see how characteristic speed and length are related could be interesting too in order to fine-tune a model according to each species.

Figure 16

Distinguishing stable and unstable geodesics is also a qualitative input when studying a surface. Stable geodesics (like the one in the middle of the surface depicted below) should have much higher chance of appearance according to our model.
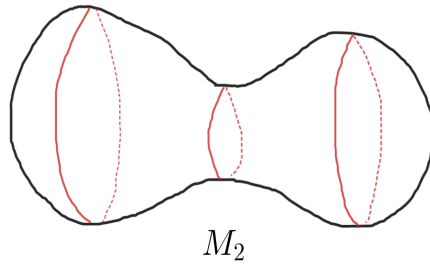

M_2

Figure 17

Finally stopping to second dimension is not mandatory. While more complicated studying 3D models (for the flesh of the apple for instance) might be worthwhile since research has yielded important results concerning the close link between nodal sets of Allen-Cahn solution and minimal hypersurfaces, see [PR03], [Pac12]. Some glance at what those surface could look like in a 3-sphere can be found in [KZ14], from where the last figure has been taken.
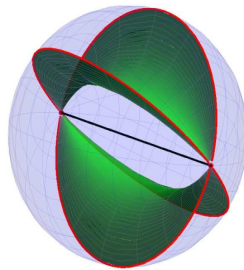

Figure 18: This figure displays a minimal surface inside a 2-sphere, with constraint that this surface must have geodesics of the sphere as boundaries. Finding such a surface is called Plateau's problem and in our case it could model the phase separation between two types of an apple chimera's flesh.

7 Conclusion

In conclusion we tried in this thesis to describe a curious biological phenomenon with mathematical tools such as differential equations or surface geometry. Although lacking empirical measures for evaluation, the model gives a good instinctive introduction to the Allen-Cahn equation and the dynamics it can induces. It also proposes a reasonable paradigm for explaining the surprising patterns that arise from some chimera plants and fruits : their phase boundaries should converge to geodesics on their surfaces, governed during the growth phase by an equation which takes into account the genetic potentials incited by both "parents".

8 Acknowledgements

This work was made possible thanks to my professor for this diploma thesis Michal Kowalczyk. Not only for sharing me the very original and exciting idea of this work, but especially for accompanying me through my progress with his mathematical knowledge and practical pieces of advice. We are grateful to his cousins, Agata and Wojciech Kowalski, for sending the photos of the apples from their orchard in Poland. I also thank Anna Godefroy for helping me on the biological part. Finally I am thankful to the University of Chile as well as the École Centrale de Nantes, for giving me the opportunity to study abroad and put into this work a sample of the various subjects of mathematics I gladly studied here in Chile during these two years.

9 Bibliography

References

[BG10]   J. W. Barrett and H. Garcke. Numerical approximation of gradient flows for closed curves in $\mathbb{R}^d$. *IMA Journal of Numerical Analysis*, 2010.

[CA77]   J. Cahn and S. Allen. A microscopic theory for domain wall motion and its experimental verification in Fe-Al alloy domain growth kinetics. *Journal de Physique, supplément au n°12, Tome 38*, 1977.

[Cho19]   O. Chodosh. Lecture notes on geometric features of the Allen-Cahn equation. Lecture, unpublished, 2019.

[dC76]   M. P. do Carmo. *Differential Geometry of Curves and Surfaces*. 1976.

[dP]   M. del Pino. Minimal surfaces and entire solutions of the Allen-Cahn equation. Lecture, unpublished.

[dPKPW10] M. del Pino, M. Kowalczyk, F. Pacard, and Juncheng Wei. Multiple-end solutions to the Allen–Cahn equation in $\mathbb{R}^2$. *Journal of Functional Analysis, 258*, 2010.

[dPKW11]   M. del Pino, M. Kowalczyk, and J. Wei. On De Giorgi conjecture in dimension $n \geq 9$. *The Annals of Mathematics, Vol. 174*, 2011.

[FC16]   M. H. Frank and D. H. Chitwood. Plant chimeras: The good, the bad, and the 'bizzaria. *Developmental Biology, 419*, 2016.

[GKH$^+$10] A. A. Green, J. R. Kennaway, A. I. Hanna, J. A. Bangham, and E. Coen. Genetic control of organ shape and tissue polarity. *PLoS Biology, Volume 8*, 2010.

[Gra89]   M. A. Grayson. Shortening embedded curves. *The Annals of Mathematics, Second Series, Vol. 129*, 1989.

[Gui]   C. Gui. Allen-Cahn equation and its generalizations. Lecture, unpublished.

[KLP12]   M. Kowalczyk, Y. Liu, and F. Pacard. The space of 4-ended solutions to the Allen-Cahn equation in the plane. *Annales de l'I.H.P. Analyse non linéaire, Tome 29*, 2012.

[KLPW14]   M. Kowalczyk, Y. Liu, F. Pacard, and Juncheng Wei. End-to-end construction for the Allen–Cahn equation in the plane. *Calculus of Variations and Partial Differential Equations, 52*, 2014.

[KZ14]   P. Krtous and A. Zelnikov. Minimal surfaces and entanglement entropy in anti-de Sitter space. *Journal of High Energy Physics*, 2014.

[lin]   https://propg.ifas.ufl.edu/03-genetic-selection/04-genetic-chimera.html.

[NHY92]   T. Noguchi, Y. Hirata, and N. Yagishita. Intervarietal and interspecific chimera formation by in vitro graft-culture method in Brassica. *Theoretical and Applied Genetics, 83*, 1992.

[Pac12]   F. Pacard. The role of minimal surfaces in the study of the Allen-Cahn equation. *Contemporary Mathematics, 572*, 2012.

[PR03]   F. Pacard and M. Ritoré. From constant mean curvature hypersurfaces to the gradient theory of phase transitions. *Journal of Differential Geometry, 64*, 2003.

[TB92]   R. A. E. Tilney-Bassett. *Plant Chimeras*. 1992.

[wika]   https://en.wikipedia.org/wiki/allen–cahn_equation.

[wikb]   https://en.wikipedia.org/wiki/curve-shortening_flow.

[wikc]   https://en.wikipedia.org/wiki/theorem_of_the_three_geodesics.